EVALUATION OF BRAIN IMAGE NONRIGID REGISTRATION ALGORITHMS BASED ON LOG-EUCLIDEAN MR-DTI CONSISTENCY MEASURES

F. J. Sánchez Castro(a)(b), O. Clatz(b), J. Dauguet(b), N. Archip(b), J.-Ph. Thiran(a), S. K. Warfield(b)

(a)École Polytechnique Fédérale de Lausanne (EPFL)
Signal Processing Institute
1015 Lausanne, Switzerland
(b)Computational Radiology Laboratory, Children's Hospital
Department of Radiology and Harvard Medical School
02115 Boston, MA, USA

ABSTRACT

Several nonrigid registration algorithms have been proposed for inter-subject alignment, used to construct statistical atlases and to identify group differences. Assessment of the accuracy of nonrigid registration algorithms is a essential and complex issue due to its intricate framework and its application-dependent behavior. We demonstrate that the diffusion MRI provides an independent means of assessing the quality of alignment achieved on the structural MRI. Diffusion tensor MRI enables the comparison of the local position and orientation of regions that appear homogeneous in conventional MRI. We carried out inter-subject alignment of conventional T1-weighted MRI with three different registration algorithms. Consequently, we projected DT-MRI of each subject through the same inter-subject transformation. The quality of the inter-subject alignment is assessed by estimating the consistency of the aligned DT-MRI using the Log-Euclidean framework.

1. INTRODUCTION

Image registration is currently used routinely in clinical environment. The fusion of information coming from different imaging modalities has revealed to be a powerful tool for a number of medical applications: radiotherapy, minimally invasive procedures, surgical navigation, robot-assisted interventions, pre-operative simulation, surgical planning, etc. The medical imaging research community has devoted substantial efforts to study the rigid and nonrigid registration problem. However, the complexity associated with the nonrigid registration makes it still an open and application-dependent problem [1]. Previous validation studies have used synthetic phantoms or landmarks correspondence to validate registration algorithms. Synthetic phantoms provide a ground truth but do not reflect the real variability observed across patients and volunteers. Landmark detection is difficult, usually time consuming and subject to inter-rater variability. Conventional inter-subject registration algorithms are usually based on structural Magnetic Resonance Images (MRI).

In this paper we propose a method to assess alignment of structural MRI using the additional information carried out by Diffusion Tensor MRI (DT-MRI). DT-MRI provides an independent and higher dimensional means of assessing the quality of the achieved registration. It enables the comparison of the local position and orientation of regions of white matter that appear homogeneous in conventional MRI. We performed inter-subject alignment of conventional T1-weighted MRI using three different registration algorithms. The DT-MRI of the same subjects were then projected using their respective computed transformations. The quality of the inter-subject alignment is assessed by estimating the deviation to the mean of the aligned DTI-MRIs using the recently proposed Log-Euclidean framework [2]. Using this approach, the tensor space is converted into a vector space allowing for group statistics (mean and variance) of the aligned tensors.

2. MATERIALS AND METHODS

2.1. Data

In this work a dataset of nine volunteers was considered. For each of them high-resolution MRI was acquired using a 3T Signa System (GE Medical Systems, Milwaukee, WI). The acquired sets of images included the following: line scan diffusion images (TR/ TE = 93/55 ms, field of view [FOV] = 270 cm, matrix size = 256×256) using a b = 1000 s/mm^2, 1 baseline (b = 5 s/mm^2) and 6 noncollinear and noncoplanar directions, 60 contiguous 2-mm-thick axial sections for each

This work was supported in part by the Swiss National Science Foundation under grant number 205320-101621, in part by NSF ITR 0426558, a research grant from CIMIT, grant RG 3478A2/2 from the NMSS, NIH grants R21 MH067054 and R01 RR021885, in part by NIH grants R03 EB006515 and U41 RR019703 and in part by a grant from la Fondation pour la Recherche Médicale.

direction; and MPRAGE 3D T1-weighted (TR/TE = 8/3.2 ms, inversion preparation time = 725 ms, postdelay time = 1400 ms, FOV = 240 cm, matrix size = 256×256), 124 contiguous 1.3-mm-thick sagittal sections.

2.2. Evaluation Strategy

A first rigid registration was carried out for each subject between the diffusion baseline image and the structural MRI to compensate for subject movement in the scanner. This estimated intra-subject transformation was then applied to the diffusion tensors (see Section 2.4 for details on the tensor reorientation).

Figure 1 gives an overview of the evaluation procedure we used.

For the inter-subject alignment, a T1-weighted MRI of a randomly chosen subject $T1_{ref}$ was used as a reference and all the other i subjects $i = 1 \dots N$ were registered to this reference. Three different registration methods were evaluated: affine, B-Splines [3] and Demons[4]. The transformations $TR_{K,i}$ estimated with each registration method were applied to the DT-MRI as described in Section 2.4. An average tensor $\bar{D}_{LOG}$ was computed at each voxel using the Log-Euclidean framework (Section 2.5). Using the same framework, the standard deviation among subjects and around the mean tensor was computed for every voxel (Section 2.5). This provides a global consistency measure for the quality of the registration algorithm tested. Additionally, the histogram of this error as a function of the quantized fractional anisotropy (FA) of the reference subject is computed to evaluate this error in regions with differing tissue structure.

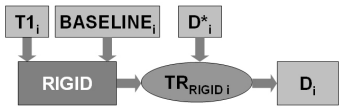

(a) Intra-subject alignment T1w-DT MRI

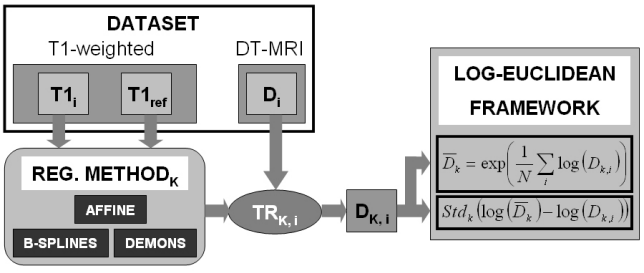

(b) Inter-subject alignment and evaluation procedure

Fig. 1. Flowcharts of the intra- and inter-subject alignment and evaluation strategy of different registration algorithms using the Log-Euclidean framework. D_i^* and D_i stands for the original DT-MRI and the DT-MRI rigidly registered with the corresponding T1-weighted respectively.

2.3. Registration Algorithms

2.3.1. Affine

A ITK [5] implementation is used. The mutual information [6] between the images to be registered is maximized by optimizing the 12 degrees of freedom (translation, rotation, scaling and shearing). The registration scheme uses a coarse-to-fine multiresolution approach and a Powell's optimization method.

2.3.2. B-Splines

A ITK [5] implementation of the free-form deformation algorithm (FFD [3]) is used. After affine initialization of the transformation, a displacement field modelled as a linear combination of B-splines is estimated by maximization of the mutual information between the images to be registered. A regular grid of uniformly distributed control points and a gradient descent optimizer were used. A coarse-to-fine pyramidal based approach was employed. At each pyramidal level, both the resolution of the images and the number of control points in each dimension were doubled. Different spacings between control points were tested to study the influence of the parameters on the tensor consistency. In this work, spacings of 40.3, 17.9, 11.5 and $8.5mm$ were tested (which corresponds to $5 \times 7 \times 7$, $10 \times 14 \times 14$, $15 \times 21 \times 21$, and $20 \times 29 \times 29$ grids of control points uniformly distributed).

2.3.3. Demons

A ITK [5] implemented multiresolution intensity-based algorithm proposed by Thirion [4], based on the concept of optical flow is used. The image alignment is approached as a diffusion process. The object boundaries in the reference image are viewed as semi-permeable membranes. The moving image is considered as a deformable grid, and diffuses through these interfaces driven by the action of effectors, called demons, situated within the membranes. The smoothness of the displacement field is controlled by filtering at each iteration with a Gaussian function of standard deviation σ. In this study σ values of 0.5, 1.0, 2.0 and 3 mm were tested to study the influence of the filtering on the results.

2.4. Reorientation of the Tensors

Unlike the univariate scalar intensity images (such as T1- and T2-weighted images), tensors are structured data and must be moved and reoriented according to the corresponding tissue deformation. It is usually assumed that the nature of the tensor should not change with the transformation [7]. Therefore, only a local rotation R should be applied to the original tensor D to compute the transformed tensor D': $D' = R^T D R$.

Assuming a transformation T that displaces a point x of the moving image to the position x' of the reference image ($x' = T(x)$), the local rotation matrix is computed using a

polar decomposition of the Jacobian matrix $J = \nabla(T)$ [7]. The Polar Decomposition theorem states that any nonsingular square matrix J can be decomposed into a rigid rotation component R and a deformation component U: $J = UR$.

2.5. Log-Euclidean Metrics and Measures of Tensor Consistency

Processing DT-MRI data has recently become of great importance in medical imaging. However, comparing tensors has revealed to be a difficult task. Euclidean metrics leads to simple computations but they can produce null or negative eigenvalues when performing operations on tensors. In addition, Euclidean averaging of tensors can also lead to a *swelling effect*, inducing artificially bigger (larger determinant) tensors than the originals [2]. Those cases are physically unrealistic.

Affine-invariant Riemannian metrics [8] have theoretical properties that overcome these problems but introduce a high computational cost. The Log-Euclidean framework [2] provides a powerful tool that allows fast computations on the tensor domain. Statistics are facilitated in this space, since computation is performed in the same way as in the Euclidean space. For details about the calculation of the matrix logarithm of a tensor see [2]. Using this framework we can compute the average tensor image of all the registered DT images using a given registration method (see section 2.2). At each voxel, an average tensor is computed as follows:

$$\bar{D}_{LOG} = \exp(\frac{1}{N}\sum_{i=1}^{N}\log(D_i)) \quad , \qquad (1)$$

where D_i stands for the registered tensor of subject i and N stands for the number of subjects. Since we are interested in the consistency of the tensors after registration the standard deviation, called error, is computed as:

$$Error = \sqrt{Trace(\frac{1}{N-1}\sum_{i=1}^{N} AA^T)} \quad , \qquad (2)$$

where $A = \log(D_i) - \log(\bar{D}_{LOG})$. $\log(\bar{D}_{LOG})$ and $\log(D_i)$ are expressed with the 6×1 vectorial representation. This produces a scalar consistency -or error- measure at each image voxel.

3. RESULTS

A color map of the consistency measure at each voxel is depicted in Figure 2 for the affine registration, B-splines algorithm with spacing between control points of $8.5mm$ and demons algorithm with regularization Gaussian filtering of $\sigma = 1mm$. The same axial slice of the 3D images is shown for the three algorithms output.

To study independently different tissues, the FA of the reference subject was quantized. The average error was also computed for every histogram bin and for every registration method. Figure 3 shows the distribution of the error for the different methods and parameters as a function of the fractional anisotropy of the reference subject. Only the voxels belonging to the brain were considered using a segmentation mask generated with Brain Extraction Tool (BET) [9].

A global consistency measure was computed for each method and each set of parameters as the mean and unbiased standard deviation of the error within the brain. These results are presented in Table 1.

The results showed that the best non-linear method (B-splines) provides a reduction of the mean global error by 16.25% and a reduction of the standard deviation of this error by 29.88% compared to affine registration. The mean global errors of the best B-splines and the best demons algorithms are comparable. However, the standard deviation of the error for the B-splines method showed a reduction by 7.22% compared to the demons method.

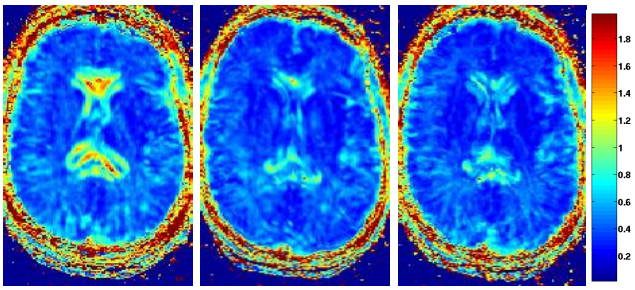

(a) (b) (c)

Fig. 2. Error to the Log-Euclidean average tensor at each voxel using different registration algorithms. (a) Affine (b) B-splines with $20 \times 29 \times 29$ control-points (c) Demons with Gaussian filtering of $\sigma = 1.0mm$.

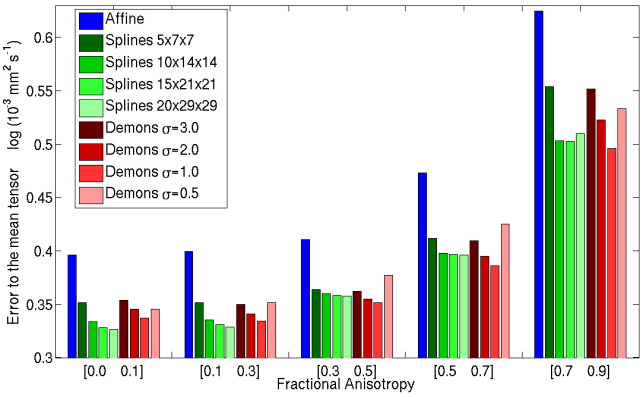

Fig. 3. Histogram of the error to the Log-Euclidean average tensor using different methods and parameters. The error is represented as a function of the quantized FA of the reference subject.

Methods	$mean \pm std$ **(**$\log(10^{-3}mm^2s^{-1})$**)**
Affine	$\mathbf{0.4105 \pm 0.1650}$
B-splines 5x7x7	0.3620 ± 0.1357
B-splines 10x14x14	0.3487 ± 0.1198
B-splines 15x21x21	0.3454 ± 0.1162
B-splines 20x29x29	$\mathbf{0.3438 \pm 0.1157}$
Demons σ=3.0	0.3605 ± 0.1406
Demons σ=2.0	0.3515 ± 0.1320
Demons σ=1.0	$\mathbf{0.3453 \pm 0.1247}$
Demons σ=0.5	0.3658 ± 0.1394

Table 1. Global error statistics. Mean and unbiased standard deviation of the error for the whole brain volume given by each method and set of parameters.

4. DISCUSSION AND CONCLUSIONS

The global increase in the error with high FA values can be explained, since the more anisotropic the tensor is, the bigger the error for the same angular misalignment gets. Moreover, since diffusion coefficients are coded as signal loss in diffusion weighted images, the regions with high FA values have a smaller signal to noise ratio, which causes the tensors to be less accurately estimated.

For the B-splines algorithm, the increase of the flexibility of the transformation (by increasing the number of control points) is consistently associated with a decrease of the mean error and standard deviation. This is explained by the good mathematical properties (C2 continuity) of the vector field modelled by B-splines functions.

The demons algorithm shows a higher sensitivity to the parameters. By decreasing the σ of the gaussian filtering regularization, the elasticity is increased and smaller mean errors are obtained. However, for small σ values, the transformation is not sufficiently constrained leading to local misalignments. This induces a re-increase of the error.

Smallest error results are obtained for the B-splines method with spacing of $8.5mm$ (20x29x29 grid) and for the demons method with a $\sigma = 1.0mm$. Figure 3 shows that for FA$<$0.3, which correspond approximately to grey matter, the B-splines algorithm performs slightly better than the demons in terms of mean error and reversely for FA$>$0.3, which corresponds approximately to white matter. However, for any FA the variance of the error for the demons algorithm is worse compared to the B-splines algorithm. As the grey matter is globally less contrasted and has a more complex structure (gyri) than the rest of the brain on the structural MRI, the regularization of the transformation plays a crucial role. White matter has more structural information and so we need a more precise point-to-point localization. In summary, the B-splines method is globally better in terms of mean error while demons registration is locally better for regions with high FA. However, demons registration is prone to have large local mismatch in some locations as shown by the increase in the standard deviation of the error for any FA.

The evaluation procedure we propose here is a general method to assess registration algorithms and to find the optimal parameters. Classical registration evaluation procedures were only based on structural MRI scalar images (1 grey value per voxel). The use of DT-MRI consistency measures provides an independent 6th order comparison means (6 independent tensor coefficients per voxel) to evaluate the quality of alignment achieved by different methods. This has allowed us to rank the different registration methods and to characterize performances of particular parameter settings.

5. REFERENCES

[1] J.P.W. Pluim, J.B.A. Maintz, and M.A. Viergever, "Mutual-information-based registration of medical images: A survey," *IEEE Transactions on Medical Imaging*, vol. 22, no. 8, pp. 986–1004, August 2003.

[2] V. Arsigny, P. Fillard, X. Pennec, and N. Ayache, "Log-euclidean metrics for fast and simple calculus on diffusion tensors," *Magn. Reson. in Medicine*, In Press, 2006.

[3] D. Rueckert, L.I. Sonoda, C. Hayes, D.L.G. Hill, M.O. Leach, and D.J. Hawkes, "Nonrigid registration using free-form deformations: Application to breast MR images," *IEEE Transactions on Medical Imaging*, vol. 18, pp. 712–721, 1999.

[4] J-P. Thirion, "Image matching as a diffusion process: an analogy with Maxwell's demons," *Medical Image Analisys*, vol. 2, pp. 243–260, 1998.

[5] L. Ibañez, W. Schroeder, L. Ng, and J. Cates, *The ITK Software Guide*, Kitware, 2nd edition, 2005.

[6] W. M. Wells, P. Viola, H. Atsumi, S. Nakajima, and R. Kikinis, "Multi-modal volume registration by maximization of mutual information," *Medical Image Analysis*, vol. 1, pp. 35–52, 1996.

[7] J. Ruiz-Alzola, C.-F. Westin, S.K. Warfield, C. Alberola, S. Maier, and R. Kikinis, "Nonrigid registration of 3d tensor medical data," *Medical Image Analysis*, vol. 6, pp. 143–161, 2002.

[8] P. G. Batchelor, M. Moakher, D. Atkinson, F. Calamante, and A. Connelly, "A rigurous framework for diffusion tensor calculus," *Magnetic Resonance in Medicine*, vol. 53, pp. 221–225, 2005.

[9] S. M. Smith, "Fast robust automated brain extraction," in *Human Brain Mapping*, 2002, pp. 143–155.